Biosensors and Bioelectronics 72 (2015) 140–147

Contents lists available at ScienceDirect

Biosensors and Bioelectronics

journal homepage: www.elsevier.com/locate/bios

Development of quantum dots-based biosensor towards on-farm detection of subclinical ketosis

Xuan Weng [a,1], Longyan Chen [a,1], Suresh Neethirajan [a,*], Todd Duffield [b]

[a] BioNano Laboratory, School of Engineering, University of Guelph, Guelph, Canada N1G 2W1
[b] Department of Population Medicine, Ontario Veterinary College, University of Guelph, Guelph, ON, Canada N1G 2W1

ARTICLE INFO

Article history:
Received 20 April 2015
Accepted 5 May 2015
Available online 6 May 2015

Keywords:
Subclinical ketosis
Quantum dots
Microfluidics
β-hydroxybutyrate

ABSTRACT

Early detection of dairy animal health issues allows the producer or veterinarian to intervene before the animals' production levels, or even survival, is threatened. An increased concentration of β-hydroxybutyrate (βHBA) is a key biomarker for diagnosis of subclinical ketosis (SCK), and provides information on the health stress in cows well before any external symptoms are observable. In this study, quantum dots (QDs) modified with cofactor nicotinamide adenine dinucleotide (NAD^+) were prepared for the sensing event, by which the βHBA concentration in the cow's blood and milk samples was determined via fluorescence analysis of the functionalized QDs. The detection was performed on a custom designed microfluidic platform combining with a low cost and miniaturized optical sensor. The sensing mechanism was first validated by a microplate reader method and then applied to the microfluidic platform. Standard βHBA solution, βHBA in blood and milk samples from cows were successfully measured by this novel technology with a detection limit at a level of 35 μM. Side by side comparison of the developed microfluidic biosensor with a commercial kit presented its good performance.

1. Introduction

When the modern dairy cow transitions from a non-lactating state to a lactating state during the periparturient period, she undergoes tremendous physiological challenges resulting in an overall state of immune suppression (Ingvartsen and Moyes, 2013). These changes are characterized by inflammatory conditions, susceptibility to metabolic disorders, uterine and mammary infections, and loss of appetite (Sordillo and Mavangira, 2014). These stresses are further complicated by the fact that the sudden initiation of an increase in milk production means that the animal is metabolically in a state of negative energy balance during the immediate postpartum period (approximately 8–10 weeks). Many of the stress symptoms that individual cows experience go unnoticed. Not only are the animals' health and welfare compromised, but there are also significant economic implications. To have reliable biomarkers of inflammatory and health status that can be routinely measured is of critical importance to detect, intervene, and manage at-risk cows as early as possible.

Subclinical ketosis (SCK) is known as elevated concentrations of circulating ketone bodies in the absence of clinical signs, has been found to be associated with high risk of clinical ketosis and displaced abomasums (Goldhawk et al., 2009). In addition, subclinically affected cows appear to have reduced milk production than those with normal ketone body concentrations (Seifi et al., 2011). The economic losses caused by SCK may be huge due to the treatment costs, decreased milk yield and decreased reproductive efficiency (McArt et al., 2011). An estimated 40–60% of cows in North America dairy herds are affected by early lactational incidence of SCK, which is much higher than the 2–15% incidence with clinical ketosis (Gordon et al., 2013; McArt et al., 2011). Determination of β-hydroxybutyrate (βHBA) is considered as the golden standard to diagnose subclinical ketosis. Cows with βHBA in their blood, milk, and urine experience a period of negative energy balance (Nydam et al., 2013). The detection of ketosis clinical signs varies, but blood βHBA concentration ranging from 1.2 to 2.9 mM is diagnosed with SCK (Iwersen et al., 2009; McArt et al., 2011; Ospina et al., 2010).

Early detection of SCK by measurement of βHBA concentration will help farmers, as these diseases generally have a poor prognosis for production and survival (Brozos et al., 2011). βHBA in cows' blood and milk are commonly used to diagnose SCK. Monitoring blood βHBA is superior to monitoring urine due to its stability (Seifi et al., 2011; Voyvoda and Erdogan, 2010). At present, such tests may be determined spectrophotometrically by traditional clinical laboratory means and would require the producer to send samples to a lab and wait for the results, which is

* Corresponding author.
E-mail address: sneethir@uoguelph.ca (S. Neethirajan).
[1] Equal contributions from the authors.

http://dx.doi.org/10.1016/j.bios.2015.05.008
0956-5663/

inconvenient, and expensive (Townsend and Eastridge, 2011). The advantage of detecting blood βHBA is that no rigorous sample handling precautions are required during the specimen transportation due to the reasonable stability of βHBA in blood. One obvious advantage of using milk instead of blood for analysis of ketosis is the non-invasive nature of milk sampling. However, because of its non-transparent nature, opacity of the sample is incompatible with spectrophotometry. Consequently, milk needs extensive pre-treatment when using traditional analytical methods, typically, precipitation, centrifugation, and special harvesting are necessary (Larsen and Nielsen, 2005; Nielsen et al., 2003). Current cow-side milk testing techniques for βHBA are not accurate and only semi-quantitative results are obtained (Larsen and Nielsen, 2005; Voyvoda and Erdogan, 2010).

Microfluidics, an emerging technology, provides new approaches for detection of toxins in food supplies (Neethirajan et al., 2011) and has been widely used in biosensor application, which is mainly used to enhance analytical performance by miniaturization. Microfluidic biosensors present distinctive advantages such as significantly increasing sensitivity, reducing assay time and sample/reagent consumptions (Mairhofer et al., 2009). Quantum dots (QDs) are semiconductor nanocrystal possessing unique optical properties due to quantum confinement effects (Algar et al., 2010). Properties such as sharp emission spectra, broad absorption spectra, higher quantum yields and tunable emission frequencies make QDs as an excellent fluorescence labels for Förster resonance energy transfer (FRET) or electron transfer (ET) processes based applications (Ma and Su, 2011). The integration of the microfluidic biochips and quantum dots (QDs) allows for capitalizing on benefits such as low analyte volume, portability, low detection limit and superior sensitivity and specificity. Quantitative detection capabilities for identification and detection of chemical species and biomarkers through the integration of a portable optical biosensor and microfluidic biochip will lead to the next generation of diagnostic devices and open up future applications.

In this study, a sensitive microfluidic biosensor was developed towards point-of-care (on-farm) sensitive detection of βHBA in serum and milk samples. As shown in Fig. 1(A), the biosensor is based on enzymatic catalysis of βHBA to acetoacetate, which concomitantly converts cofactor nicotinamide adenine dinucleotide (NAD^+) to its reduced form β-nicotinamide adenine dinucleotide (NADH). The NAD^+ here is pre-conjugated with fluorescent nanoparticles quantum dots (QDs). The NAD^+ has been reported to partially quench the fluorescence of the conjugated QDs through an electron transfer (ET) process (Akshath et al., 2012; Freeman and Willner, 2008), while the reduced form NADH has no effect on QDs fluorescence. The change of fluorescent intensity from cofactor conjugated QDs can indicate the change of βHBA concentration in samples. By further coupling with a microfluidic platform with optical detection unit, this biosensor is capable of providing a rapid and accurate measurement of βHBA from a small volume of blood and milk samples.

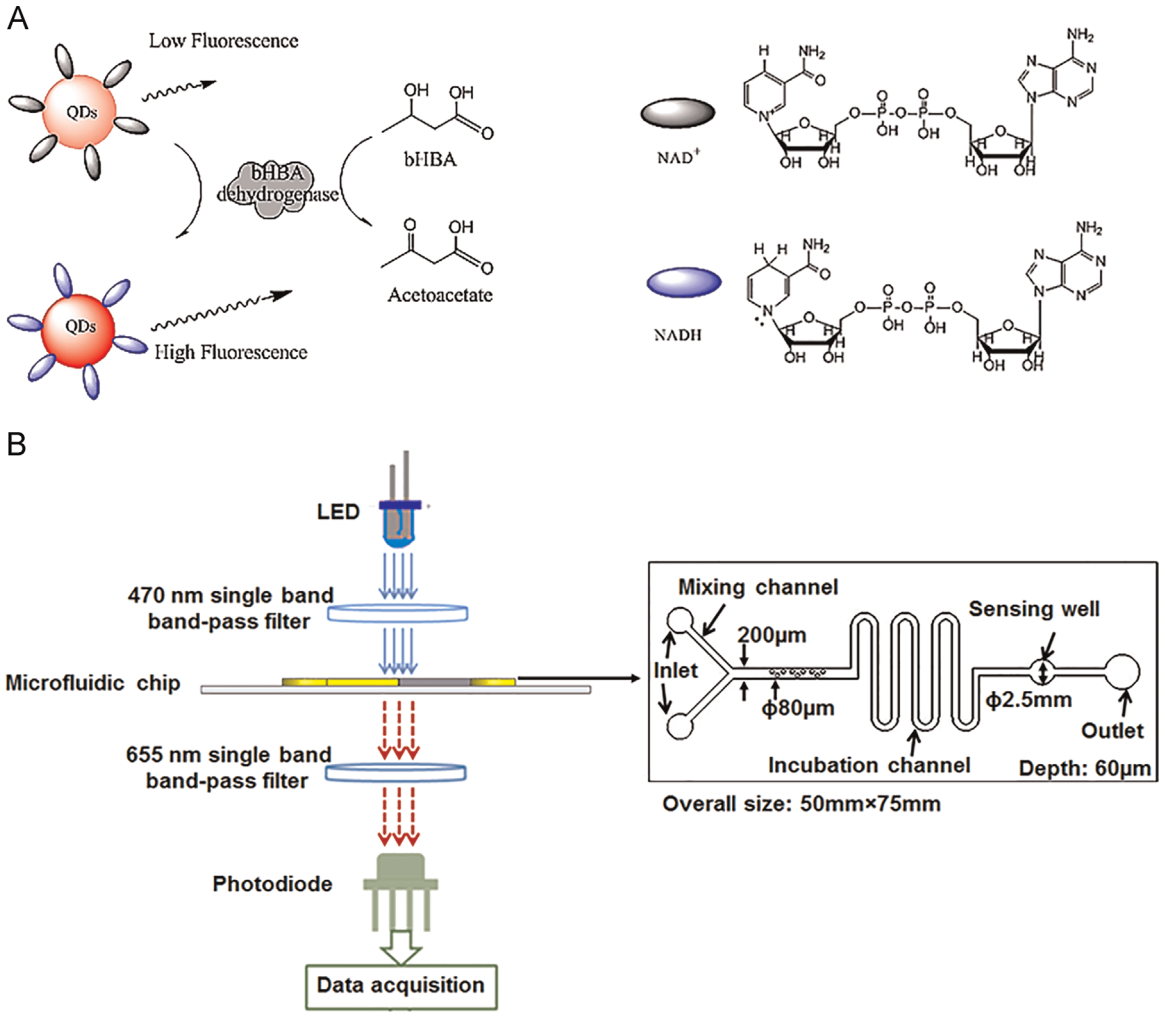

Fig. 1. (A) Schematic illustration of sensing mechanism. (B) Sketch of microfluidic platform combining with the low-cost, miniaturized optical sensor.

2. Materials and methods

2.1. Reagents and sample preparation

β-hydroxybutyric acid, nicotinamide adenine dinucleotide (NAD^+), β-Nicotinamide adenine dinucleotide, reduced (NADH), 3-aminophenylboronic acid monohydrate (APBA), N-(3-dimethylaminopropyl)-N′-ethylcarbodiimide hydrochloride (EDC), bovine serum albumin (BSA), Tetrahydrofuran (THF) and phosphate-buffered saline (PBS) were purchased from Sigma-Aldrich Canada (Oakville, ON, Canada). β-hydroxybutyrate dehydrogenase was ordered from Roche Diagnostics (Laval, Quebec, Canada). All reagents were of analytical reagent grade. Carboxyl quantum dots were purchased from life technologies (Qdot® 655 ITK™ Burlington, ON, Canada). Milk was purchased from a local grocery store.

The βHBA standard solution ranging from 1.6 μM to 1000 μM was made by diluting the 3-hydroxybutyric acid with PBS buffer and was used for the βHBA standard curve. Serum samples with known βHBA concentration analyzed by using a Roche Cobas 6000 c501 automated chemistry analyzer (Roche Canada, Laval, QC, Canada) were provided by our collaborator (Ontario Veterinary College, Canada) and the detailed sample preparation procedure can be found elsewhere (Gohary et al., 2014). Briefly, cow's blood was firstly collected from the coccygeal blood vessels in a vacuum tube without anticoagulant and stored in a cool place. Collected sample was then centrifuged to harvest serum at 4 °C within 6 h after collection at 2990*g* and stored at −20 °C for further use. Before assaying, the serum sample was thawed at room temperature and diluted to a series of concentration ranging from 10 μM to 1000 μM with PBS buffer. Milk was centrifuged at room temperature at 2300*g* for 3 min twice and then the suspension was removed. Fortified milk sample solutions were prepared by spiking βHBA concentration ranging from 0 to 1000 μM to the centrifuged milk for further use.

2.2. Preparation of functionalized QDs nanoprobes

To prepare NAD^+-/NADH-functionalized QDs, commercialized carboxyl group capped QD nanoparticles were firstly modified with 3-aminophenyl boronic acid (APBA) through carbodiimide reaction. In a typical preparation, 50 μL of 8 μM stock solution of carboxyl QDs was mixed with 50 μL of 10 mg/mL of APBA dispersed in PBS/THF solution (v/v, 1/1). After 3 min of gentle shaking, 25 μL of 10 mg/mL of N-(3-dimethylaminopropyl)-N′-ethylcarbodiimide hydrochloride (EDC) was added. The volume of the mixture was then brought to 1 mL by adding PBS. The solution was incubated at room temperature for 2 h under gently shaking. Afterwards, the resultant particles were purified through ultrafiltration (Amicon Ultra-0.5 mL centrifugal filters, MWCO 100 kDa, EMD Millipore Inc.). The nanoparticles were then re-suspended in 1 mL of PBS and kept at dark for further use.

For NAD^+/NADH conjugation, the purified APBA-QDs nanoparticles were further mixed with NAD^+/NADH with a feeding molar ratio of APBA-QDs to NAD^+/NADH of 1/60000 for 1 h at room temperature. The cofactor conjugated QDs were purified by ultra-filtration and re-suspended in PBS to a final concentration of 0.4 μM. The NAD^+-/NADH-QDs solutions were stored at 4 °C under dark for further use.

2.3. Preparation of microfluidic chip

The detailed information about the design and preparation of the microfluidic chip can be found in our previous work (Weng et al., 2014). Briefly, the microfluidic chip consisted of a mixing channel housing with hundreds of posts which were used to enhance mixing effect, incubation channel, sensing well, two inlets and one outlet, as shown in Fig. 1(B). Flow in the microchannel was driven by capillary force (Hitzbleck et al., 2012; Mohammed and Desmulliez, 2014) hence avoided mechanical or electrical micropumps. This capillary-driven pumpless approach facilitates the development of a disposable on-site diagnostic system. Here, the reagent and the sample solutions must be loaded into the two inlets simultaneously to maximally avoid trapping air bubble. Cylinder-shaped posts were embedded in the microchannel as the passive micromixer which has been proven to be able to enhance mixing performance without damaging bio-cells in the transmission (Alam et al., 2014). The microfluidic chip was made by the following the standard soft lithography protocol (Weng et al., 2011). The fabrication involved making a silicon wafer master by depositing a 60 μm layer of UV cured SU-8 2025 negative photoresist (MicroCHEM, USA) onto the surface of the wafer to form a master mold bearing the desired microchannel layout. A microfluidic chip was formed in the master mold from a degassed mixture of PDMS prepolymer and curing agent (10:1 w/w, Sylgard, Dow Corning, Burlington, ON, Canada) after curing for 4 h at 75 °C. Solidified PDMS replica was then peeled off the master mold, being punched to form the inlets and outlet and bonded onto a glass slide ($25 \times 75 \times 1$ mm^3, VWR International, Suwanee, GA, USA) after oxygen plasma treatment for 40 s. A position marker was used to facilitate the alignment between the sensing well and the sensing window of the photodiode mounted in a custom-built container ($10 \times 6 \times 5$ cm^3) when conducting the bonding. A schematic of the custom-built container for optical and electrical components assembly and alignment can be found in Fig. S1, in which labels 1–5 indicate the positions for mounting LED, excitation bandpass filter, microfluidic chip, emission bandpass filter and Si photodiode, respectively.

2.4. Characterization

The morphology of quantum dots nanoprobes were characterized by A Philips CM-10 transmission electron microscope (TEM) operating at 120 kV. The hydrodynamic diameters, size distribution and Zeta (ξ) potentials of the cofactor conjugated QDs were measured in water by a dynamic light scattering (DLS) system (Malvern Zetasizer Nano ZS, UK). A Synergy H4 Hybrid Multi-Mode Microplate Reader (Biotek, Winooski, VT, USA) was used to perform the validation of the mechanism of the QDs-based biosensor.

2.5. Evaluation of sensing performance and detection of βHBA in microplate reader

The QDs-based biosensor was validated by conducting the reaction on a dark microplate (Greiner CELLSTAR®, Sigma-Aldrich, Canada) and performed the optical analysis with top reading by the Synergy H4 microplate reader mentioned above. In a typical validation experiment, βHBA standard solution with concentration ranging from 1.6 μM to 1000 μM was prepared by diluted from the 10 M β-hydroxybutyric acid solution. The enzyme solution was made fresh before each experiment by diluting β-hydroxybutyrate dehydrogenase at a ratio of 1:50. NAD^+-QDs and BSA (1%) were mixed at a ratio of 1:5 (v/v). For each experiment in the microwell, 20 μL of βHBA standard solutions, 12 μL of mixture of NAD^+-QDs and bovine serum album (BSA), 10 μL of enzyme solution were mixed together. Then the mixture was brought to 100 μL in total by adding 58 μL PBS to minimize the optical detection errors caused by the uneven liquid surface. Three replicates of each standard were made. The microplate with the solution mixtures was then covered by aluminum foil for protection from light followed by incubation at room temperature for 30 min. After the

incubation, the fluorescence spectra of the resultant complex were analyzed by the microplate reader (Ex: 470 nm, Em: 655 nm). Serum sample and fortified milk sample were measured by following the same procedure. Each data point represents two separate experiments conducted in triplicate.

2.6. Device apparatus and detection of βHBA by microfluidic sensor

A custom designed miniaturized optical sensor integrated with the microfluidic platform developed in our previous work (Weng et al., 2014) was built to achieve the fluorescence signal analysis. The optical and the electrical components were selected considering the stability of the sensor response for high performance. The optical sensor was made of a high brightness LED (470 nm, Luxeon Rebel, Luxeon Star LEDs, Brantford, ON, Canada) and a single-band bandpass filters of 470 nm (semrock, Rochester, NY, USA), mounted on cool base with enhanced thermal stability providing the excitation light, and a single-band bandpass filters of 655 nm (semrock, Rochester, NY, USA) and a low noise, high sensitivity photodiode (Hamamatsu, Bridgewater, NJ, USA) capturing the fluorescence illumination from QDs. The light signal was then digitized and transferred to a computer for storage and further analysis by a programmable microcontroller (Arduino Uno, SparkFun Electronics, Niwot, CO, USA) with an interface circuit consisting of several functional units in between. The configuration of the microfluidic platform and the optical sensor is shown in Fig. 1(B).

The experiment by the custom designed optical sensor followed the procedure described below. A series of βHBA standard solutions with concentration of 1.6 μM, 8.0 μM, 40 μM, 200 μM and 1000 μM were measured. In a typical test, 3 μL of mixture containing βHBA standard solution (diluted serum sample or fortified milk sample), mixture of NAD^+-QDs and BSA (v/v, 1:5) and 3 μL fresh made 3-hydroxybutyrate dehydrogenase enzyme solution were added into the inlets of the microfluidic chip simultaneously. After the mixture flew into the sensing well, fluorescence signals were monitored every minute for a total time of 7 min. For both microplate reader based assay and microfluidic assay, the detection limits were calculated as recommended by IUPAC (Thomsen et al., 2003) by using standard deviation of the standard deviation of blank measures and sensitivities.

To further evaluate the performance of the microfluidic biosensor, a batch of serum sample with known concentration (723 μM, 1266 μM, 1476 μM, 2141 μM and 3005 μM) analyzed by the chemistry analyzer was detected side by side with a commercial kit (Cayman Chemical® β-Hydroxybutyrate (ketone Body) Colorimetric Assay kit, Cedarlane labs, Burlington, ON, Canada). Before an assay, the serum sample was thawed at room temperature and diluted to 1:6. Three replicates of each standard and diluted serum sample were prepared and measured; the average absorbance readout by the microplate reader was calculated to evaluate the sample concentration. Similarly, each sample was tested for 3 times by the microfluidic biosensor; the average voltage output of the photodiode was then calculated to determine the sample concentration.

3. Results and discussion

3.1. Characterization of QDs nanoprobes

To prepare cofactor-QDs nanoprobes, carboxyl QDs was conjugated with APBA via carbodiimide reaction. The cofactors NAD^+ (or NADH) was further immobilized to APBA conjugated QDs by phenylboronic acid groups involved cyclic esters reaction (Ferrier and Prasad, 1965). As shown in Fig. 2(A), the successful immobilization of cofactor QDs nanoprobes was demonstrated by observing increasing of absorbance intensity at 259 nm for both NAD^+-QDs and NADH-QDs comparing to bare QD with same concentration. A weak spectrum shoulder (dark arrow) could be observed at 340 nm for NADH-QDs, which is another characteristic absorption peak for NADH. We also demonstrated the conjugation of NADH to QDs by observing the emission peak at 460 nm under excitation at 340 nm from NADH-QDs as shown in Fig. 2(B) (shown in the small window). Based on the emission intensity of NADH, we were able to determine the number of NADH per QD. As indicated in Fig. S2A, the number of NADH per QD was found to be $\sim 1532 \pm 122$. This number is significantly higher than that reported in literature (~40 per QD) (Freeman and Willner, 2008), where QDs was capped with glutathione through the interaction of single –SH group to ZnS shell. The colloidal stability of alkanothiol capped QDs may be poor, due to desorption of the ligands from nanoparticles (Aldana et al., 2001). Commercial QDs we used here which are likely coated with a layer of polymer, which greatly promote the particle water solubility and present larger amount of carboxylic group on the surface for further conjugation (Pellegrino et al., 2004). NAD^+ does not emit fluorescence. However, due to the similarity of chemical structure (ribose), it is estimated that same number of NAD^+ has been conjugated per QD. TEM image (Fig. S3A) shows the cone-like shape of NAD^+-QDs nanoprobes. The average hydrodynamic diameter of NAD^+-QDs was determined to be ~26 nm by DLS measurement (Fig. S3A, bottom

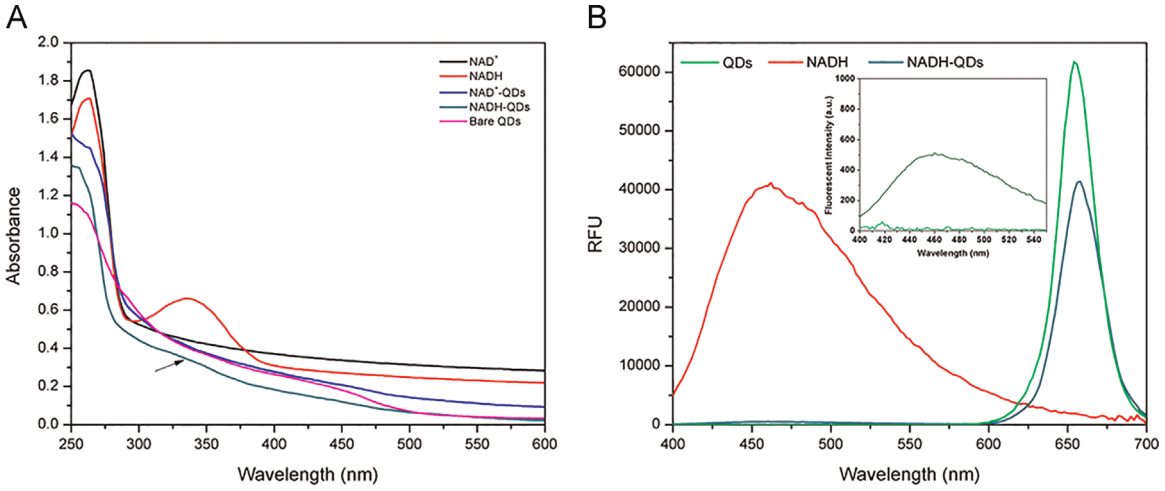

Fig. 2. (A) UV–visible spectra and (B) fluorescence spectra of cofactors and nanoprobes.

left). The cofactor conjugated nanoprobes show moderate dispersion in aqueous medium, as indicated from the Zeta potential data (Fig. S3B). The Zeta potential (ζ) values of NAD^+-QDs and NADH-QDs are -27.9 ± 7.81 mV and -28 ± 7.01, respectively, which indicate the moderate dispersion of the cofactor conjugated nanoprobes in aqueous medium (Greenwood and Kendall, 1999; Hanaor et al., 2012).

3.2. Evaluation of sensing mechanism

NAD^+ was known as an important co-factor for over 300 dehydrogenases in the metabolic pathways. In a typical NAD^+-involved enzyme reaction, it acts as a redox electron carrier to accept electrons and gets transferred to its reduced form NADH. NAD^+ has been reported to effectively quench the fluorescent emission of QDs (Freeman and Willner, 2008). The fluorescence quenching of QDs by NAD^+ has been attributed to an electron (charge) transfer process (Freeman and Willner, 2008; Ren et al., 2010). In this process, the energy generated from the excited state in QDs is transferred to the extra carrier, NAD^+, via a non-radiative recombination, instead of emitting photons to generate fluorescence (Akshath et al., 2012). As a result, this non-radiative recombination is much larger than the radiative electron–hole recombination and hence was followed by the process of quenching the fluorescence (Akshath et al., 2012).

As shown in Fig. 3(A), we were able to find higher quenching of fluorescence intensity by comparing the emission profile from the two cofactors conjugated nanoprobes with the same concentration. To further evaluate the effect of cofactors to fluorescence of QDs, we performed a competition binding test by adding excess amount of free NAD^+ (15 mM) to NADH-QDs (200 nM), and vice versa. Fig. 3(B) shows that the QDs emission at 655 nm decreases in the presence of NAD^+, which could be attributed to the replacement of NADH binding on the surface of QDs by NAD^+ molecules. Meanwhile, addition of NADH in NAD^+-QD results in the recovery of fluorescent intensity. Based on the higher ratio of fluorescence recovery by NADH than that of quenching by NAD^+, it is probable that the NADH may have higher binding affinity to APBA molecule on the surface of QDs.

The stability of cyclic esters formed through the binding of APBA to diols group (NADH or NAD^+) is pH dependent. The optimum pH range for the binding is reported in physiological condition (~pH 7) (Springsteen and Wang, 2002), which potentially stabilizes our assay. Thus the assay pH was strictly controlled in our experiment. In addition, the presence of cis-diols containing molecules such as sugars may compete with cofactors to bind onto QDs as indicated through competition test. However, it should be noted this requires large amount of sugar molecules. A typical sample dilution process could eliminate the interferences. In addition, free NAD+ has been reported to quench the fluorescence of CdTe QDs through the same charge transfer process by diffusing onto the surface of QDs (Akshath et al., 2012). The assay signal may not be largely affected due to the replacement of NAD+ by small amount of sugars from the conjugation of QDs.

3.3. Detection of βHBA in microplate reader

We then evaluated the use of the NAD^+-QDs nanoprobes for βHBA detection. The enzymatic oxidation of the major ketone body βHBA is expected to convert NAD^+-QDs to NADH-QDs, which consequently results in proportional increasing of QDs emission intensity (at 655 nm). Fig. 4(A) shows the fluorescence spectra upon the reaction of the NAD^+-modified QDs with variable concentrations of βHBA in the presence of βHBA dehydrogenase. As the concentration of βHBA increases, the fluorescence intensity of QDs increases due to the formation of more amount of NADH on QDs from NAD^+. βHBA concentrations in the samples were determined by analysis of the varying intensities of the fluorescence output from the sensor. Fig. 4(B) demonstrates the fluorescence intensities of the QDs at 655 nm which were dependent on the concentrations of βHBA. As the concentration of βHBA increases, the fluorescence intensity increases accordingly due to the higher amount of NADH-QDs were converted from NAD^+-QDs. An R^2 value of 0.9511 was found for linear response region between 8 μM and 1000 μM with a detection limit of 1.2 μM. In the experiment, a control experiment without loading βHBA was done for comparison. It is concluded that the βHBA dehydrogenase had no effect on the fluorescence of the QDs. Therefore, this NAD^+-modified QDs enable us to differential the βHBA concentration.

Serum samples with known βHBA concentration and the fortified milk samples spiked with βHBA standards were then mixed with NAD^+-functionalized QDs, and the QDs emission intensity was analyzed by the microplate reader. As shown in Fig. 4(C) and (D), different βHBA concentrations in both the serum sample and the fortified milk samples are well differentiated based on the

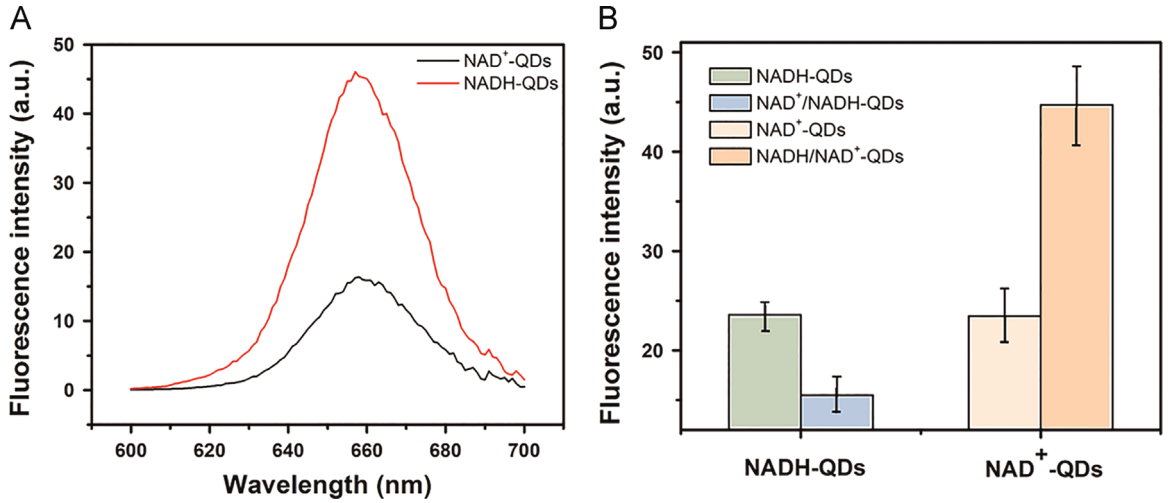

Fig. 3. (A) Fluorescence spectra of NAD^+-functionalized QDs and NADH-functionalized QDs (λ_{ex}=470 nm). (B) Fluorescence intensity at 655 nm for a mixture of NAD^+ and NADH-functionalized QDs, and NADH and NAD^+-functionalized QDs.

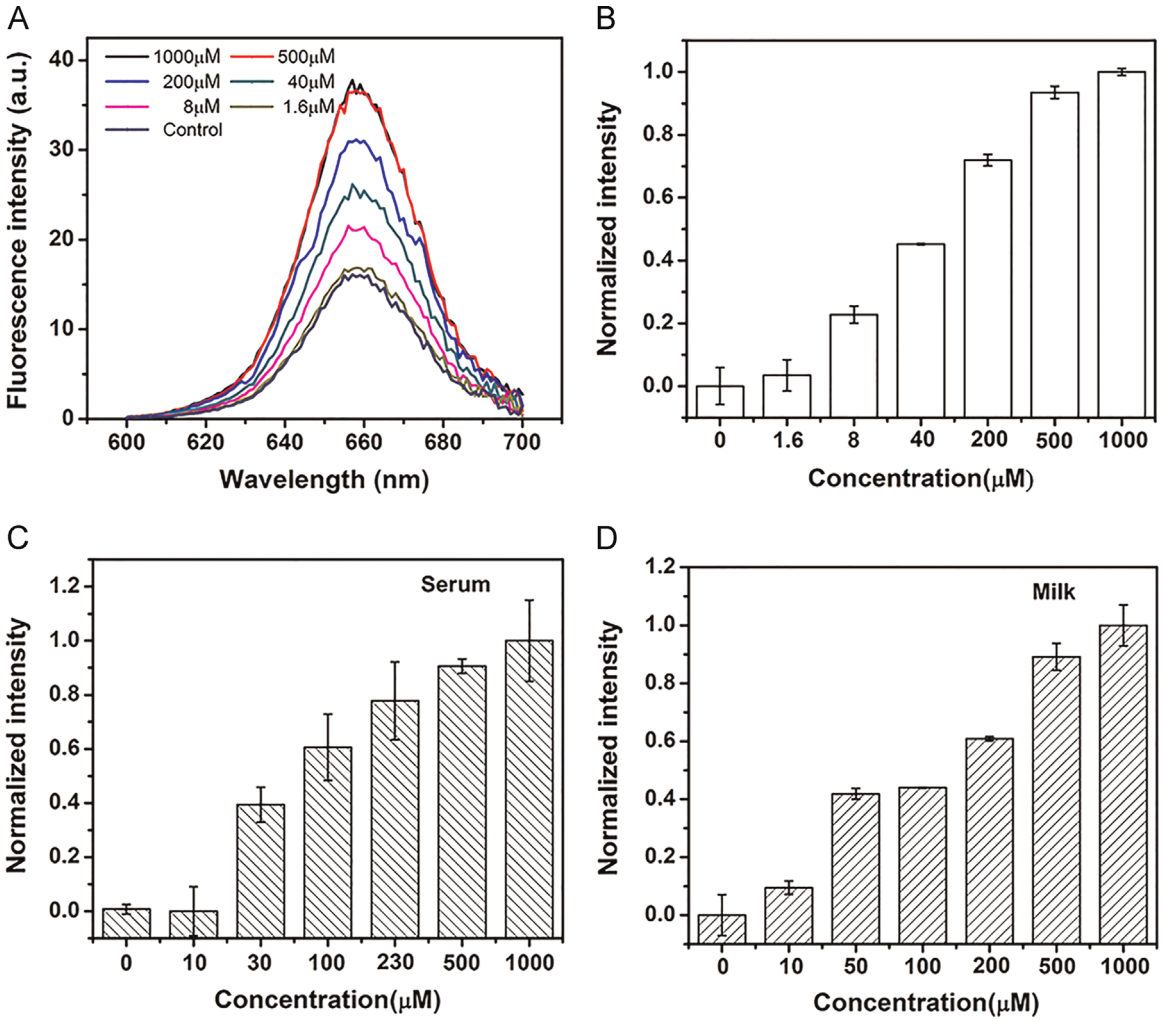

Fig. 4. (A) Fluorescence spectra upon the reaction of NAD^+ functionalized QDs with a series of βHBA standard solution. (B) Fluorescence intensity at 655 nm of variable concentrations of βHBA by NAD^+ functionalized QDs. (C) Fluorescence spectra upon the reaction of NAD^+ functionalized QDs with a series of diluted serum sample. (D) Fluorescence spectra upon the reaction of NAD^+ functionalized QDs with a series of fortified milk sample.

changes of fluorescent intensity. No significant fluorescent signal interference due to complex matrix in milk samples was observed during the experiments. The obvious advantage of this fluorometric method is that no tedious pre-treatment is required to obtain a transparent status for milk, therefore, contamination and disturbance caused by precipitating step may be avoided. In conclusion, the presented fluorometric determination of βHBA based on NAD^+-functionalized QDs is a valid method for analysis of serum or milk.

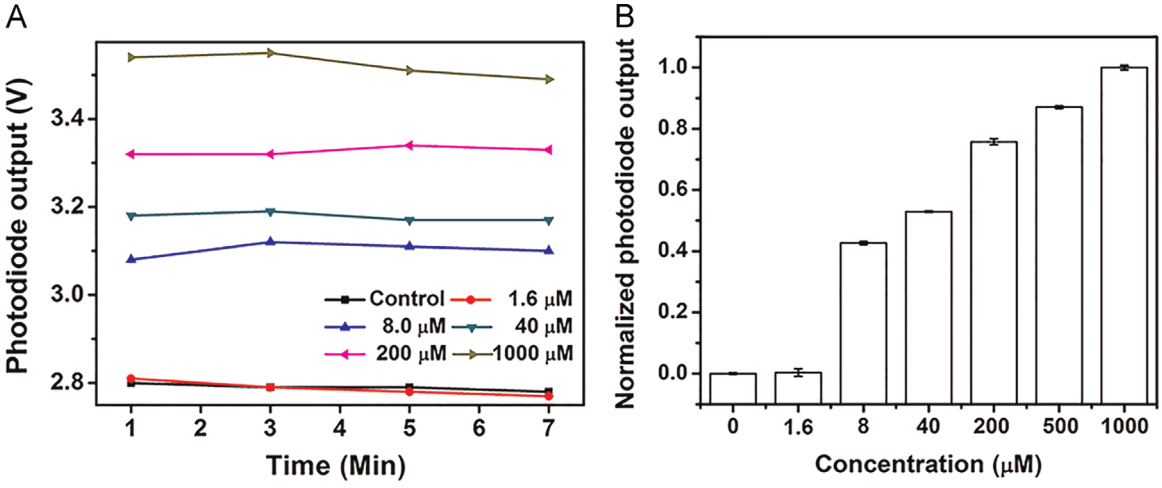

Fig. 5. (A) Time-dependent response of biosensor with a series of βHBA standard solution. (B) Normalized photodiode output of biosensor in measurement of the standard βHBA concentration.

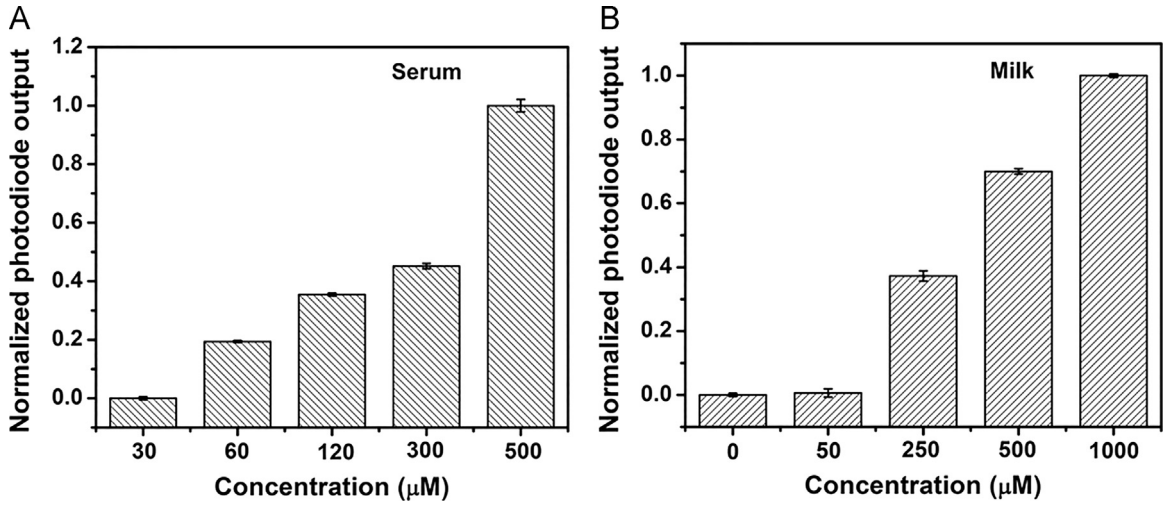

Fig. 6. (A) Normalized photodiode output of biosensor in measurement of the βHBA concentration in diluted serum samples. (B) Normalized photodiode output of biosensor in measurement of the βHBA concentration in fortified milk samples.

3.4. Detection of βHBA by microfluidic biosensor

βHBA standard solution, serum samples from dairy cows, and fortified milk samples were measured on the microfluidic biosensor. Firstly, the time-dependent fluorescence changes upon the reaction of NAD^+-functionalized QDs with βHBA standard solution were investigated, which is shown in Fig. 5. Fluorescence intensity was measured and recorded at the end of the first minute after mixing and then every other minute with a total period of 7 min. The result demonstrates that the changes of fluorescence intensity for all standard solutions are not distinguishable after 3 min, which indicated the completion of the enzymatic reaction. Therefore, 3 min was taken as the sufficient incubation time for the microfluidic biosensor and used in the following experiments of preparation of βHBA standard curve, serum and milk sample measurement. Fig. 5(B) demonstrates the fluorescence intensities reflected by the output of photodiode depending on the interaction between the NAD^+-functionalized QDs with variable βHBA standard solution for a fixed time interval of 3 min. As the concentration of βHBA increases, the output of the photodiode increases, which indicates the fluorescence intensity of the QDs is intensified. An R^2 value of 0.9728 was found for linear response region between 8 μM and 1000 μM with detection limits of 35 μM. This result is consistent of the formation of higher amount of NADH-QDs. Serum samples with known βHBA concentration and the fortified milk samples were measured by this biosensor, the results are shown in Fig. 6. Both of the serum and milk samples are easily distinguished based on the changes of βHBA concentration. Good repeatability was observed in both sample tests. The calculated detection limit for the serum sample was 34.8 μM, which highly agrees with that of standard solution with linear regression of 0.9423. For the milk sample, detection limit and the linear regression were 40.3 μM and 0.9658, respectively. Both of the results present the good performance of the presented microfluidic biosensor βHBA detection in blood and milk samples. In addition, when compared to the blood detection, a slightly poor detection limit was observed, which may be caused by the interference of the complex matrix in milk. This may be improved via further processing of the milk sample by centrifugation. The stability of this biosensor has been confirmed by the small standard derivative of the data point presented in the plots. The comparison of the microfluidic biosensor with the commercial kit was shown in Table S1.

4. Conclusions

In this study, we present a QDs-based biosensor for the detection of βHBA towards on-farm subclinical ketosis diagnosis. The use of NAD^+ functionalized QDs as fluorescent labels offers superior performance for the βHBA sensing event. Conducting the measurement on a microfluidics platform significantly decreases the sample/reagent consumption and detection time due to the small scale and high surface area to volume ratio of the microchannel structure, which is a distinctive advantage over many commercially available kits (Cayman Chemical® β-Hydroxybutyrate (Ketone Body) Colorimetric Assay Kit; MaxDiscovery™ β-Hydroxybutyrate Assay Kit) which usually require relative big volumes of sample/reagent or bulky, expensive spectrophotometric equipment. Custom-built miniaturized and low-cost optical biosensor provides high sensitivity in QDs fluorescence analysis. Both milk and serum sample from dairy cows were measured and quantitative results were achieved, for a typical test, result could be obtained in 3 min with a detection limit of 35 μM. Good agreement in serum detection has been confirmed upon side by side comparison with a commercial kit. A promising capability of measuring milk βHBA by the microfluidic biosensor was implicit by the presented result although no comparison with a commercial kit was conducted as only semi-quantitative analysis for milk βHBA was found on the market. Although some handheld meters designed for human medicine (Precision Xtra™) have been employed for cowside SCK diagnosis and reported to have good sensitivity and specificity, but provides significantly false positive results, and can analyze only the blood samples. The dual-sample detection capability is another advantage for the presented microfluidic biosensor. The developed quantum dots-based microfluidic biosensor for subclinical ketosis detection is designed as a specific portable device towards on-farm and cowside diagnosis of SCK, which provides a framework towards the delivery of improved dairy animal health management solutions in Canada and around the world.

Acknowledgments

The authors sincerely thank the Natural Sciences and Engineering Research Council of Canada (Grant number 400929), the Canada Foundation for Innovation (Grant number 500512) and the Dairy Farmers of Ontario (Grant number 051520) for funding this study.

Appendix A. Supplementary Information

Supplementary data associated with this article can be found in the online version at http://dx.doi.org/10.1016/j.bios.2015.05.008.

References

Akshath, U.S., Vinayaka, A.C., Thakur, M.S., 2012. Biosens. Bioelectron. 38, 411–415.
Alam, A., Afzal, A., Kim, K., 2014. Chem. Eng. Res. Des. 92, 423–434.
Aldana, J., Wang, Y.A., Peng, X., 2001. J. Am. Chem. Soc. 123, 8844–8850.
Algar, W.R., Tavares, A.J., Krull, U.J., 2010. Anal. Chim. Acta 673, 1–25.
Brozos, C., Mavrogianni, V.S., Fthenakis, G.C., 2011. Vet. Clin. N. Am.-Food 27, 105–113.
Ferrier, R.J., Prasad, D., 1965. J. Chem. Soc. 1, 7429–7432.
Freeman, R., Willner, I., 2008. Nano Lett. 9 (1), 322–326.
Gohary, K., LeBlanc, S.J., Lissemore, K.D., Overton, M.W., von Massow, M., Duffield, T. F., 2014. J. Dairy Sci. 97, 6231–6241.
Goldhawk, C., Chapinal, N., Veira, D.M., Weary, D.M., von Keyserlingk, M.A.G., 2009. J. Dairy Sci. 92, 4971–4977.
Gordon, J.L., LeBlanc, S.J., Duffield, T.F., 2013. Vet. Clin. N. Am.-Food 29, 433–445.
Greenwood, R., Kendall, K., 1999. J. Eur. Ceram. Soc. 19, 479–488.
Hanaor, D.A.H., Michelazzi, M., Leonelli, C., Sorrell, C.C., 2012. J. Eur. Ceram. Soc. 32, 235–244.
Hitzbleck, M., Avrain, L., Smekens, V., Lovchik, R.D., Mertens, P., Delamarche, E., 2012. Lab Chip 12, 1972–1978.
Ingvartsen, K.L., Moyes, K., 2013. Animal 7 (S1), 112–122.
Iwersen, M., Falkenberg, U., Voigtsberger, R., Forderung, D., Heuwieser, W., 2009. J. Dairy Sci. 92, 2618–2624.
Larsen, T., Nielsen, N.I., 2005. J. Dairy Sci. 88, 2004–2009.
Ma, Q., Su, X., 2011. Analyst 136, 4883–4893.
Mairhofer, J., Roppert, K., Ertl, P., 2009. Sensors 9, 4804–4823.
McArt, J.A.A., Nydam, D.V., Ospina, P.A., Oetzel, G.R., 2011. J. Dairy Sci. 94, 6011–6020.
Mohammed, M.I., Desmulliez, M.P.Y., 2014. Biosens. Bioelectron. 61, 478–484.
Neethirajan, S., Kobayashi, I., Nakajima, M., Wu, D., Nandagopal, S., Lin, F., 2011. Lab Chip 11, 1574–1586.
Nielsen, N.I., Ingvartsen, K.L., Larsen, T., 2003. J. Vet. Med. A 50, 88–97.
Nydam D.V., Ospina P.A., McArt J.A., Oetzel G., Overton T.R., Eastridge M.L., 2013. In Proceedings of the 22nd Tri-State Dairy Nutrition Conference, Fort Wayne, Indiana, USA, pp. 9–22.
Ospina, P.A., Nydam, D.V., Stokol, T., Overton, T.R., 2010. J. Dairy Sci. 93, 546–554.
Pellegrino, T., Manna, L., Kudera, S., Liedl, T., Koktysh, D., Rogach, A.L., Keller, S., Rädler, J., Natile, G., Parak, W.J., 2004. Nano Lett. 4, 703–707.
Ren, X., Yang, L., Tang, F., Yan, C., Ren, J., 2010. Biosens. Bioelectron. 26, 271–274.
Seifi, H.A., LeBlanc, S.J., Leslie, K.E., Duffield, T.F., 2011. Vet. J. 188, 216–220.
Sordillo, L.M., Mavangira, V., 2014. Anim. Prod. Sci. 54, 1204–1214.
Springsteen, G., Wang, B., 2002. Tetrahedron 58, 5291–5300.
Thomsen, V., Schatzlein, D., Mercuro, D., 2003. Spectroscopy 18, 112–114.
Townsend, J., Eastridge, M.L., 2011. In: Proceedings of the 20th Annual Tri-State Dairy Nutrition Conference, Grand Wayne Center, Fort Wayne, Indiana, USA, pp. 55–60.
Voyvoda, H., Erdogan, H., 2010. Res. Vet. Sci. 89, 344–351.
Weng, X., Jiang, H., Chon, C.H., Chen, S., Cao, H., Li, D., 2011. J. Biotechnol. 155, 330–337.
Weng, X., Zhao, W., Neethirajan, S., Duffield, T., 2014. J. Nanobiotechnol. 13, 13.